NUREG/CR-4264
LA-10436-MS

Los Alamos National Laboratory is operated by the University of California for the United States Department of Energy under contract W-7405-ENG-36.

Investigation of High-Efficiency Particulate Air Filter Plugging by Combustion Aerosols

Los Alamos National Laboratory
Los Alamos, New Mexico 87545

8507050422 850531
PDR NUREG
CR-4264 R PDR

An Affirmative Action/Equal Opportunity Employer

Edited by M. C. Timmers, Group Q-6
Prepared by O. E. Garnica, Group Q-6

NOTICE

This report was prepared as an account of work sponsored by an agency of the United States Government. Neither the United States Government nor any agency thereof, or any of their employees, makes any warranty, expressed or implied, or assumes any legal liability or responsibility for any third party's use, or the results of such use, of any information, apparatus, product or process disclosed in this report, or represents that its use by such third party would not infringe privately owned rights.

NUREG/CR-4264
LA-10436-MS

RI

Investigation of High-Efficiency Particulate Air Filter Plugging by Combustion Aerosols

D. L. Fenton*
M. V. Gunaji*
W. S. Gregory
R. A. Martin

Manuscript submitted: April 1985
Date published: May 1985

Prepared for
Division of Risk Analysis
Office of Nuclear Regulatory Research
US Nuclear Regulatory Commission
Washington, DC 20555

NRC FIN No. A7029

*Mechanical Engineering Department, New Mexico State University, Las Cruces, NM 88003.

Los Alamos National Laboratory
Los Alamos, New Mexico 87545

INVESTIGATION OF HIGH-EFFICIENCY PARTICULATE AIR FILTER PLUGGING BY COMBUSTION AEROSOLS

by

D. L. Fenton, M. V. Gunaji,
W. S. Gregory, and R. A. Martin

ABSTRACT

Experiments were conducted to investigate high-efficiency particulate air (HEPA) filter plugging by combustion aerosols. These tests were done to obtain empirical data to improve our modeling of filter plugging phenomena using the Los Alamos National Laboratory fire accident analysis code FIRAC. Commercially available 0.61-m by 0.61-m square filters were tested in a specially designed facility to determine how airflow resistance varies with increased filter loading by combustion aerosols. Two organic fuels normally found in nuclear fuel cycle facilities, polystyrene (PS) and polymethylmethacrylate (PMMA), were burned under varied conditions to generate combustion aerosols. The test facility included a combustor, a 23-m-long duct, and a specially designed gravimetric balance for determining the aerosol mass gain of the filters.

Test results include correlations of HEPA filter resistance ratios (actual resistance/initial resistance) with aerosol mass gain. The mass gain of plugged HEPA filters was found to correlate with the airborne mass concentration of material in the size range greater than approximately 2.0 μm. Also, the fuel with a smaller soot fraction, PMMA, produced filter plugging at lower accumulated aerosol mass deposits on or within the filter.

I. INTRODUCTION

High-efficiency particulate air (HEPA) filters are used commonly in nuclear reactor or fuel processing plant ventilation systems to protect the outside environment and plant workers from airborne radioactive particles. Additional applications include hospitals, where bacteria-free atmospheres are required for operating rooms, and numerous other facilities where clean air is necessary.[1]

Exposing a HEPA filter to heat and smoke significantly alters its operating characteristics. This investigation focuses on the characteristics related to

filter plugging or the increase in pressure drop across a filter as a result of the collection of particulate material on the filtration media. Such information is required to better understand how filters are plugged with combustion-generated aerosols and will improve our estimates of ventilation system response to compartment fires using an existing Los Alamos fire accident analysis computer code called FIRAC.

II. OBJECTIVES

An experiment that provided the required HEPA filter plugging data and was based on the combustion of two solid fuels was designed. The fuels we selected bracketed the particle material generation rate (the mass fraction of the solid fuel that converts to aerosol particles) that would be expected in a typical nuclear facility.[2] The two fuels selected were polystyrene (PS) and polymethylmethacrylate (PMMA); their soot fractions are nominally 0.33 and 0.021, respectively. For these numbers, both the soot and low vapor pressure liquids are included in the aerosolized combustion product mass normalized by the unburned fuel mass for overventilated conditions.[3] We had six specific questions about the problem we investigated.

(1) What is the correlation between accumulated combustion particulate mass on the HEPA filter and flow resistance across the filter?
(2) What is the effect of soot fraction (as manifested by fuel type) on HEPA filter plugging?
(3) What is the effect of the fuel mass burning rate on HEPA filter plugging?
(4) How far do the aerosols penetrate within the filtration medium?
(5) Does the HEPA filter upstream faceguard influence filter plugging?
(6) What is the magnitude of particle deposition within the duct upstream from the HEPA filter?

The experimental work was directed at answering these questions. The equipment included a combustion chamber where the fuels were burned, an airflow facility composed of a fan and duct, and a specially designed gravimetric balance with an accuracy of 2 to 3 g for measuring the accumulated mass collected by the HEPA filter.

III. FILTRATION AND PLUGGING THEORY

Filtration involves the capture of airborne particles by a filter's medium. Analysis of particle capture treats the medium as a long cylinder folded upon itself a number of times. Short-range mechanisms of particle capture by a long circular cylinder include inertial impaction, interception, and diffusion.[4]

A. Inertial Impaction

If an individual particle moving with uniform velocity is introduced in a fluid ahead of a circular cylinder, it will tend to follow the streamlines. However, because the particle necessarily must have mass, the particle motion may diverge from that of the streamline and possibly hit the circular cylinder. The actual deviation of particle motion from the fluid streamlines is greater for particles of larger mass and for higher-velocity flows.

B. Interception

With the inertial impaction mechanism, it was assumed that the particle has mass but no size, but in interception the assumption made is that the particle has no mass but has a finite size. Thus, the particle approaching a cylinder will not diverge from the fluid streamlines. Interception of the particle will occur when the distance between the cylinder surface and particle center is not greater than the radius of the particle.

C. Diffusion

Particles that are submicron in size rarely are collected by inertial impaction or interception because they are small and can follow the streamlines or move across them in a zigzag way. This zigzag movement is caused by continued and irregular bombardment of the molecules of the fluid and is called Brownian motion. The capture of aerosols by diffusion is more likely when the free stream velocity is low and the particles are very small ($d < 1\ \mu m$).

D. Combination of Filtration Mechanisms

Real particles have a definite mass and size; hence, the inertial impaction and interception mechanisms do not act independently. It is more likely that two or more mechanisms act in combination, with one dominating over the other. For example, with particles in the micron size range and larger, inertial impaction and interception will dominate, whereas diffusion is likely to dominate for submicron-sized particles.

E. Effects of High Temperature on Particle Collection Mechanisms

The effect of high temperature on the particle collection mechanisms was studied by Thring and Strauss.[5] With an increase in temperature, the efficiency of collection by interception and inertial impaction decreases but that by diffusion increases. This increase in filtration efficiency by diffusion is a result of the increased level of Brownian motion at increased temperatures.

F. Filter Resistance

The resistance of HEPA filters to flow is defined as[6]

$$W = \frac{\Delta P}{Q} \quad , \tag{1}$$

where ΔP is pressure drop across the filter in centimeters water gauge and Q is the flow rate in cubic meters per hour. The relative resistance is defined to be W/W_o, where W_o is the clean filter resistance, $\Delta P_o/Q_o$.

Based on the resistance of cylinders placed parallel to the flow, an expression for the pressure drop is[6]

$$\Delta P = \frac{4\beta\eta\phi Qb}{Ar_f^2} \quad , \tag{2}$$

where η is the coefficient of fluid dynamic viscosity (Newton-second per square meter), β is the packing density of fibers, Q is the flow rate (cubic meters per second), A is the face area of the filter (square meters), ϕ is given by $\left(-\ln\beta + 2\beta - \frac{\beta^2}{2} - \frac{3}{2}\right)^{-1}$, b is the filter thickness (meters), and r_f is the mean fiber radius (meters). The factor β is incorporated because the fibers are perpendicular to the airflow. Usually, the value of β ranges from -0.5 to 1.5.

In calculating the flow resistance of HEPA filters, the parameters used are

ΔP, pressure drop;

Q, flow rate;

A, area;

b, thickness of the filter;

η, coefficient of dynamic viscosity of the fluid,

ρ, density of fluid,

λ, microscopic mean free path of the fluid molecules, and

r_f, mean fiber radius.

Davies did a dimensional analysis coupled with experiments[5,7] and gave the following expression for the pressure drop.

$$\Delta P = \frac{16\eta Q b \beta^{1.5}}{A r_f^2}\left(b + 1 + 56\beta^3\right) , \qquad (3)$$

where the quantities η, Q, b, β, A, and r_f are defined the same as for Eq. (2). Davies stated that Eq. (3) is valid for packing densities (β) less than 0.02. For filters with higher packing densities, he gave the following expression for pressure drop.

$$\Delta P = \frac{17.5\eta Q \beta^{1.5} b(1 - \beta)(1 + 52\beta^3)}{A r_{fe}^2} , \qquad (4)$$

where η, Q, b, β, and A are same as for Eq. (2), but r_{fe} is the effective fiber radius.

G. Filter Plugging

Filter plugging involves the deposition of solid particles on fibers, which changes the filter's operational characteristics. This deposition causes an increase in the flow resistance of the filter. There may be considerable changes in the filtration characteristics while the deposition of solid particles is building up and the filter is becoming plugged. The deposited particles may not distribute evenly over the surface of the fibers but may act as very fine fibers themselves by constructing chain structures, which results in an increase of filtration efficiency.[6]

The change in flow resistance across the filter because of plugging depends on the following factors.[7]

(1) Particle Phase. Aerosols of liquid droplets wet the filter and may draw fibers together by capillary action, increase pore size, and decrease both filter resistance and efficiency. Thus, liquid aerosols will cause a smaller change in flow resistance than solid particle aerosols. The penetration of liquid aerosols has been found to increase with time.[6]

(2) Particle Size. Smaller particles usually cause a higher flow resistance than larger particles for a given total particulate mass.[8]

(3) Filter Structure. Depending on the filter structure, the particles are deposited either on the face of the filter or inside it. The penetration of the particles into the filter depends on the air velocity and filter structure.

(4) Mass of Collected Particles. This is related to the unit area of the filter. The pressure drop across the filter increases with increasing particle loading on the filter. It may be considered as the sum of filter pressure drop and the pressure drop of a layer consisting of the deposited particles.[7]

1. Dendrite Model. C. Tien et al.[9] put forward a theory for the formation and growth of particle dendrites on a collector placed in an aerosol stream. The theory is based on (1) the finite size and (2) the randomness of the location of particles (aerosols) in the fluid stream. Tien made the assumption that the particle trajectory depends only on the particle inertia and the drag force.

Because of the finiteness of the particle size, shadowing and chain deposition effects become important. When a particle is deposited on a fiber surface, protrusion above the surface occurs, providing greater surface area than before. There is greater chance for the capture of subsequent particles because of the increased surface area. When these subsequent particles are captured by particles that were deposited earlier, a chainlike particle dendrite is formed. This process proceeds with the dendrite having a greater surface than before and consequently greater possibility of particle capture.

In this model of filter plugging, there is a region on the fiber surface called a shadow where no particles can deposit. Thus, the capture of particles by the interception mechanism occurs, which implies the assumption that particle deposits do not disturb the airflow streamlines.

W. Bergman et al.[10] assumed that the pressure drops resulting from the filter fibers and the particle dendrites are independent and, when added, give the pressure drop across the filter. They derived the following expression for a filter consisting of fibers and particle dendrites.

$$\Delta P = \Delta P_o \left(1 + \frac{R_f \alpha_p}{r \alpha_f}\right)\left(1 + \frac{R_f^2 \alpha_p}{r^2 \alpha_f}\right)^{1/2} \quad . \tag{5}$$

Equation (5) also can be used for a filter having two discrete fiber sizes. The pressure drop, ΔP_o, is given by

$$\Delta P_o = \eta V A b \left(\frac{16 \alpha_f^{3/2}}{R_f^2}\right) \quad . \tag{6}$$

The parameters involved in Eqs. (5) and (6) are

η, coefficient of fluid dynamic viscosity;
V, fluid velocity;
b, filter thickness;
R_f, fiber radius;
r, particle dendrite radius;
α_p, volume fraction of the trapped particles; and
α_f, fiber volume fraction.

Bergman et al. further simplified Eq. (5) for low particle loading by neglecting the nonlinear part. Consequently, Eq. (5) reduces to

$$\Delta P = \Delta P_o \left(1 + \frac{R_f \alpha_p}{r \alpha_f}\right) \quad . \tag{7}$$

Equation (7) predicts the increased pressure drop because of particle loading will be inversely proportional to the particle size.

2. Increasing Fiber Model. Bergman et al.[10] also assumed that the particles form a deposit that increases the fiber's size without changing its shape. On the basis of deposit geometry, they gave the following expression for the increase in fiber radius (R_f).

$$R_f = R_o\left(1 + \frac{12\alpha_p}{\pi\alpha_f}\right)^{1/2} , \tag{8}$$

where R_o is the original fiber radius and α_p and α_f are the same as before. Using

$$\Delta P = \Delta P_o\left(\frac{R_f}{R_o}\right) \tag{9}$$

for pressure drop, Eq. (8) can be rearranged to yield

$$\Delta P = \Delta P_o\left(1 + \frac{12\alpha_p}{\pi\alpha_f}\right)^{1/2} , \tag{10}$$

where ΔP_o is defined by Eq. (7). Comparing Eqs. (5) and (10) indicates that pressure drop for the increasing fiber model is less than the pressure drop for the dendrite model with the same particle volume deposited on the filter.

For filters undergoing realistic plugging conditions, Bergman et al.[10] state that the mechanisms of the increasing fiber and particle dendrite models might act in combination. At very low particle loadings on the filter, the increasing fiber model gives a major contribution, but after a small amount of loading, the dendrite model prevails. They concluded that the dendrite and increasing fiber models are limiting cases of a more general filter plugging model.

3. Phenomenological Model. Previous filter plugging tests with dry stearic acid aerosol[11,12] strongly discredit the two models described earlier; evidence of discrepancies also is given in Bergman's work.[10] Rather than trying to construct any realistic physical mechanism for the cause of plugging, we propose a phenomenological approach; namely, we assume the following relation.

$$\frac{W}{W_o} = F\ (M_p) \quad , \tag{11}$$

where W is the resistance coefficient defined in Eq. (1) and W_o is the value of W for a clean filter. F is a monotonically increasing function of M_p, which is the total mass of particulate accumulated on the filter, and is the relative resistance. To satisfy the clean filter requirement, we must have

$$F\ (M_p = 0) = 1 \quad . \tag{12}$$

We believe the following expression should be adequate for all practical purposes.

$$F = 1 + \alpha M_p + \beta M_p^2 \quad , \tag{13}$$

where α and β are two coefficients determined by experimentation. Their evaluation forms the basis of the filter plugging test program.

IV. MODIFIED HEPA FILTER LOADING FACILITY

The existing HEPA filter loading facility was modified to accommodate the requirements associated with combustion aerosol generation and filter plugging experiments. The original filter loading facility is described in Ref. 11 and Ref. 12. Specifically, the modifications included the addition of the solid fuel combustor, the installation of a turbulent mixing grid, the construction and

installation of a metal duct, and the addition of approximately 7.4 m of straight duct upstream from the test filter location.

Size 5 HEPA filters, which have a nominal airflow capacity of 1690 m^3/h, face dimensions of 0.61 by 0.61 m, and a depth of 0.292 m, were tested in this investigation.[13] The unplugged filters had a mass of approximately 16 kg. The Mine Safety Appliance Corporation manufactured the HEPA filters tested.

A. Air-Handling Equipment and HEPA Filter Test Section

The air-handling equipment and HEPA filter test section are described in detail elsewhere.[11,12] We will discuss only the features used for combustion aerosol experiments. For example, 2.4 m of stainless-steel duct was installed immediately downstream from the HEPA filter prefilter to facilitate addition of the test fuel combustor. A turbulence mixing grid was added at the downstream edge of this steel duct to disperse the combustion products over the duct airflow. The grid was composed of 2.2-cm-o.d. copper tubing spaced approximately 5.08 cm apart center to center.

Two pressure measurements were required. The first was the static pressure drop across the HEPA filter. Four static pressure taps were located at the center of each duct wall 0.45 m upstream or downstream from the filter face; a Dwyer vertical manometer capable of a 1-mm-w.g. resolution was used to measure the static pressure drop. The second pressure measured was the centerline velocity pressure; a Dwyer inclined manometer capable of a 0.005-cm-w.g. resolution was used. The centerline velocity was measured with a pitot-static probe in the circular cross-section duct downstream from the HEPA filter test section. Horizontal and vertical traverses across the circular duct yielded velocity profiles that were used to calculate the volumetric flow rate of the air. A centerline coefficient that relates the volumetric airflow rate to the centerline velocity then was determined. Repeating these calculations for the volumetric flows expected in a typical HEPA filter plugging test relates the centerline velocity to the volumetric airflow rate. Figure 1 shows the centerline coefficient as a function of volumetric flow where the coefficient Y is given by the equation $Y = 0.8320 + 0.00004618(Q) - 1.065 \times 10^{-8} Q^2$, where Q is the volumetric flow rate. The centerline coefficient was used to determine all the volumetric airflows.

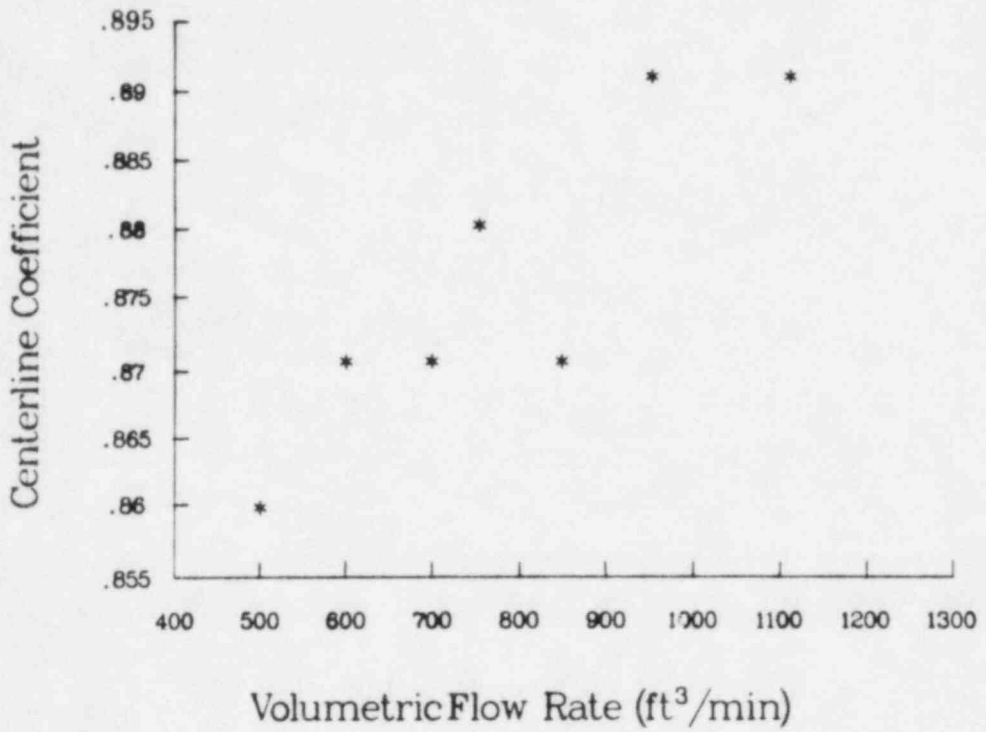

Fig. 1.
Centerline coefficient as a function of volumetric flow.

Air temperature measurements were made at five positions, and the inlet and outlet dry and wet bulb temperatures were measured with a psychrometer. Copper-constantan (type T) thermocouples were used to measure the temperature of the airflow at the branch section and upstream and downstream of the test HEPA filter. A thermocouple digital temperature indicator was used to monitor the thermocouples, which were accurate to $\pm 0.5\ ^{o}C$ at the 95% confidence level.

The measurements made at the filter test section included particulate mass on the filter, pressure drop across the filter, particulate mass concentration, and particle size distribution.

B. Test Fuel Combustion

The test fuels (PS and PMMA) were burned in a combustor designed at Battelle Pacific Northwest Laboratory. Figure 2 is an assembly drawing of the combustor. The burner was positioned on the underside of the stainless-steel duct immediately downstream from the HEPA prefilter and secured by a flanged steel pipe section using eight 0.79-cm-diam bolts.

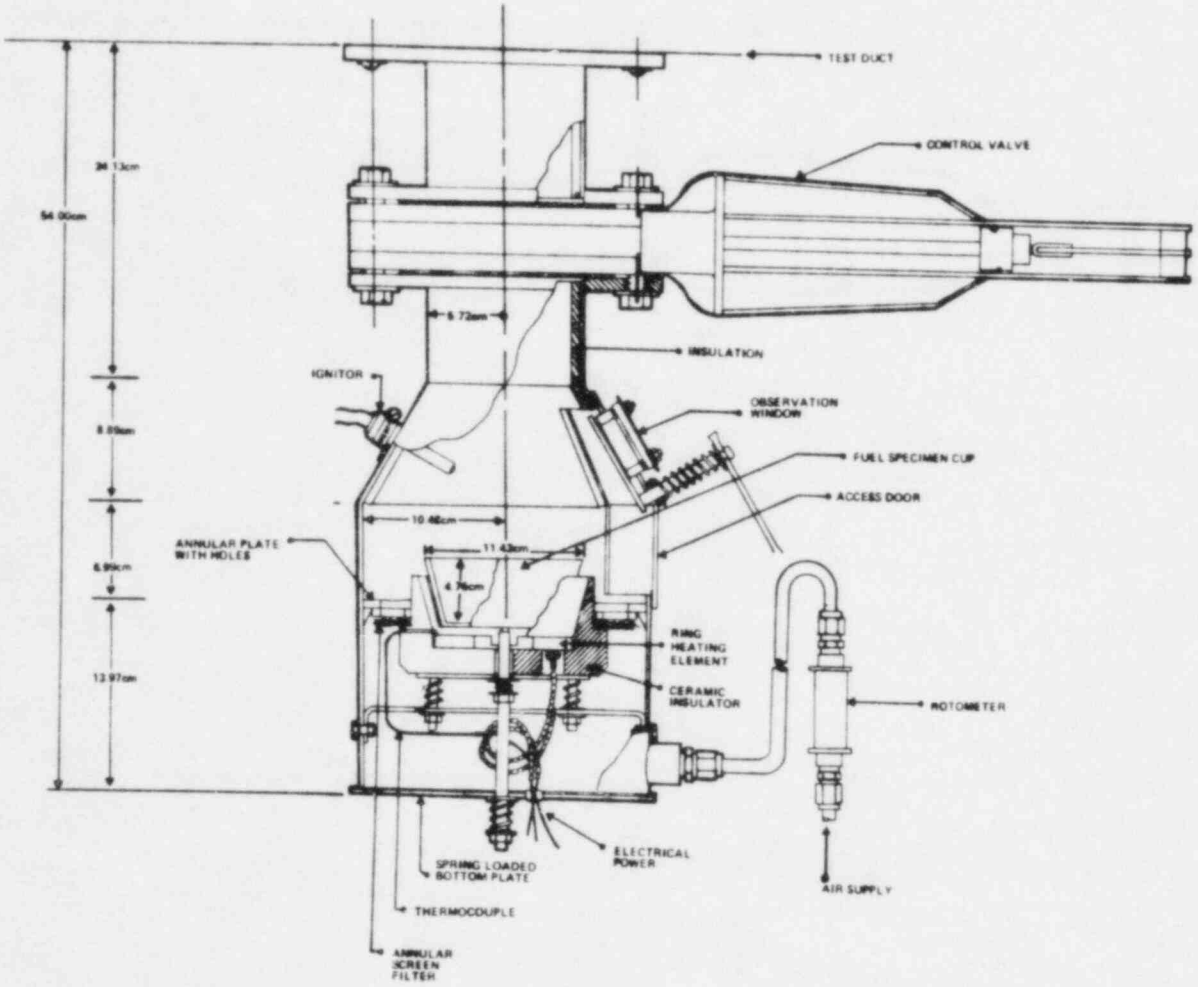

Fig. 2.
Assembly drawing of the combustor.

A major feature of the combustor is a cup holder where the fuel was contained and heated. The chamber walls provided the capability of performing combustion in a positive pressure atmosphere (the duct interior). Fuel preheat temperatures were nominally 500^{o}C and were achieved by a 400-W electrical ring heater controlled by a Chromalox on-off temperature controller. The flame was diffusion-controlled, and the burning rate was regulated by adjusting the airflow rate to the combustor by means of a valve and rotameter. A gate valve at the top of the burner (under the stainless-steel duct) was maintained in the full-open position after the fire was started.

C. Combustion Product Characterization

Characterization of the combustion products included only the particulate constituents. The combustion products were not monitored continuously; samples were taken from time to time and were considered adequate.

Particulate mass concentration (milligrams per cubic meter) was determined with Anderson Mark III stainless-steel, in-stack, inertial impactors incorporating straight nozzles. These impactors also measured aerodynamic particle diameter (based on unit density spheres) through seven stages of particle collection and a back-up filter. Preimpactors for use in conjunction with the impactors were determined to be unnecessary for this application. Real-time particle sizing equipment also was used (a Royco Model 225 Aerosol Particle Counter and a TSI Model 3030 Electrical Aerosol Analyzer). The real-time equipment was used intermittently to determine the particle size characteristics and mass concentration variation with the burn time. The optical counter sized particles simultaneously in all the ranges and thus was suitable for monitoring changing concentrations. However, the Electrical Aerosol Analyzer sized particles sequentially over a cycle time of about 3 min and thus was not able to characterize the aerosol accurately. In contrast, the inertial impactors were operated in such a manner (nozzle diameter and sampling time) to sample over the entire fuel burn period--up to 20 min. For this reason, the impactor size data were chosen for application to the HEPA filter plugging studies.

V. EXPERIMENTAL PROCEDURES

The fuels tested required essentially the same test procedures, which are as follows.

(1) Each filter was examined for holes by observing it against a light source. The filter frame was checked for squareness, which was necessary to prevent leaks at the flexible duct HEPA filter flange.

(2) The test fuel cups were weighed when empty and then with the fuel sample so that the mass was known for determining the apparent burning rate. The cups were placed on a hot plate with the temperature automatically kept at 500°C (932°F).

(3) An aluminum plate (7.8 by 7.8 by 0.2 cm) was attached to the bottom of the HEPA filter being tested to provide a smooth load cell contact point.

(4) The HEPA filter was placed on the pneumatic cylinders, raised, and attached to the gravimetric balance beam assembly with four screws.

(5) The force transducer assembly was positioned under the filter and bolted to the support structure. The direct current power supply was adjusted to +15 Vdc, maintained at this level for all the filter tests, and never turned off. This was done to achieve steady-state operation of the power supply. The pneumatic cylinders then were lowered.

(6) The HEPA filter was nulled or balanced by adjusting the counterweights on the gravimetric balance assembly. The filter was considered nulled if the output of the transducer was in the range of 20 to 40 mV.

(7) Calibrating the force transducer involved placing known weights on the nulled filter and recording the output. The output was recorded from two to four times and then averaged for each known weight. The calibration equation was determined at the conclusion of the HEPA filter plugging test.

(8) The pneumatic cylinders were raised, forcing the HEPA filter against the stops. This was the filter's position for operation and particulate loading. The flexible ducts then were clamped around the filter.

(9) The test fuel cup ring heater (within the combustor) was switched on, and the Chromalox on-off controller was adjusted to 500°C. Approximately 40 min were required for the cup to achieve the set temperature. During this time interval, the fan prefilter was changed, all electronic instruments were rechecked, and the pressure manometers were adjusted for correct zeros.

(10) The airflow facility fan was turned on.

(11) The barometric pressure was recorded and corrected for temperature and local elevation.

(12) The airflow adjusting door located at the fan box was adjusted to yield the desired velocity pressure (volumetric airflow) measured in the circular cross-section duct downstream from the test HEPA filter.

(13) Temperatures at the inlet, at the branch (downstream from combustor), upstream from test HEPA filter, downstream from HEPA filter, and at the exit were recorded. The static pressure drop across the filter also was recorded.

(14) The airflow facility fan was turned off to start the fire. The fuel test cup was placed in the combustor cup holder, and the top gate valve was opened slightly. No air was supplied to the combuster, which allowed vapors to accumulate in the volume above the cup. After 5--10 min, the igniter coil was energized electrically. (Fuel vapor ignition occurred most consistently in this manner.) After combustion was initiated, the top gate valve was moved to full open, and the combustion airflow was adjusted to the required flow (0.00047 or 0.0019 m^3/s) on the rotameter by means of a valve.

(15) The airflow facility fan was switched on, and the thermocouple temperature measurements were recorded after ~10 min had elapsed.

(16) The data acquisition process involved the following items.

- The time at which the flame first appeared was recorded.
- The time at which the flame disappeared was recorded.
- After flame disappearance, the top gate valve was closed, and the inlet and exit dry and wet bulb temperatures, HEPA filter static pressure drop, and velocity pressure in tne circular cross-section duct were recorded.
- The airflow facility fan was turned off, the test HEPA filter was released from the flexible duct, and the pneumatic cylinders were lowered. The force transducer zero output was recorded. The HEPA filter was lowered carefully onto the force transducer so that no horizontal forces were present, and the output was recorded. The HEPA filter weight gain measurement was repeated four times.

(17) The HEPA filter was returned to the test position by raising the pneumatic cylinders and reinstalling the flexible duct.

(18) The next fuel test cup was placed inside the combustor and the vapors were ignited as before.

(19) The above procedure was repeated until the volumetric airflow rate was reduced to one-half of the initial flow rate, 845 m^3/min, that is, fully plugged conditions. This condition was assumed as fully plugged, and the test was concluded.

The difference between procedures used for PS and PMMA combustion involves the ignition of the fuel and the number of cups burned between data recordings. For PS, the ignition technique used the heating coil as described above. However, a propane torch was used in place of the coil for ignition for the PMMA

fuel. One cup of PS fuel was burned between data recordings, whereas from three to five cups of PMMA fuel were burned to obtain an appropriate mass gain on the HEPA filter.

VI. EXPERIMENTAL RESULTS

Table I is a summary of the conditions associated with the combustion of the test fuels. The stoichiometric airflow rate was based on the given fuel chemistry and the apparent fuel mass burning rate observed during preliminary tests.

The experimental results and the analyses are presented for the PS and PMMA HEPA filter plugging tests. Separate sections are used for the discussions because of the difference in the soot fraction with combustion of the two fuels. Physical characterization of the particulate material is presented first; then the HEPA filter plugging data are discussed. Experimental results on smoke transport and deposition [see question (6) in Sec. II] are reported elsewhere (Ref. 14).

A. PS Combustion and HEPA Filter Plugging

Cascade impactors were used to measure both total particulate mass concentration and particle size on the basis of aerodynamic diameter.[14] Figure 3 shows the PS particle size measurements directly upstream from the HEPA filter and gives the particulate mass concentrations at the same location. Note that for both the high and low mass burning rates, the particle size distribution is

TABLE I

TEST FUEL COMBUSTION CONDITIONS

Fuel	Chemical Formula	Combustion Efficiency	Stoichiometric Airflow Rate (m^3/h)	Ratio of Actual to Stoichiometric Airflow Rates	Comments
PS (granular)	CH	0.6	7.4	0.23	Low Burn Rate, Underventilated
				0.93	High Burn Rate, Underventilated
PMMA	$CH_{1.6}O_{0.4}$	0.9	4.0	0.85	Low Burn Rate, Underventilated
				2.1	High Burn Rate, Overventilated

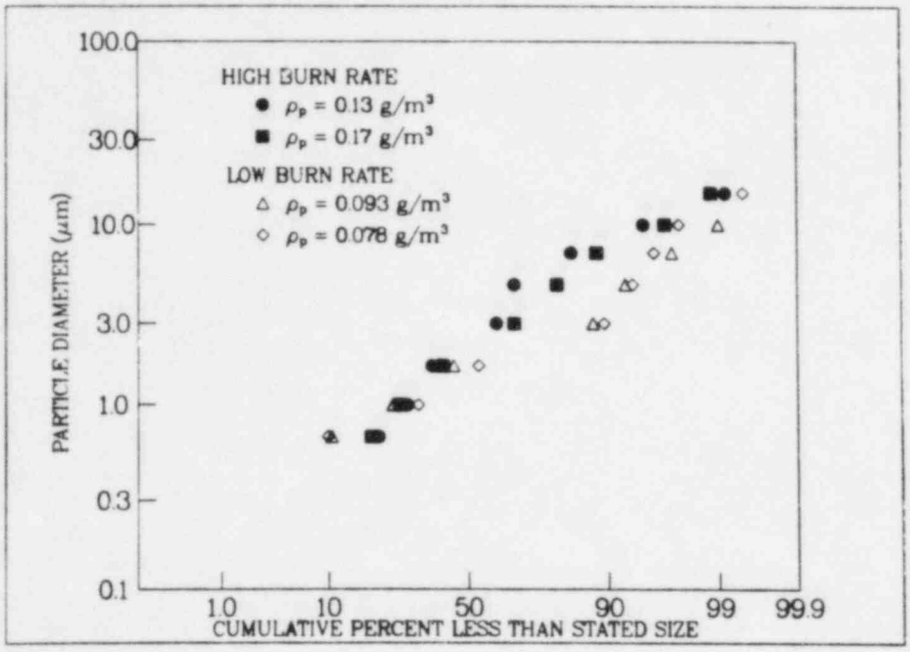

Fig. 3.
Polystyrene combustion particulate mass size distribution.

nearly the same for particles less than 2.0 μm. However, for particle diameters greater than 2.0 μm there is a significantly greater relative number of particles at the higher burning rate compared with the lower burning rate.

The particulate mass concentration data, in conjunction with the mass burning rate data, imply an important feature associated with PS combustion. This feature is that the total particulate mass concentration measured near the HEPA filter is proportional to the mass burning rate. This is established by ratioing the average high burning rate to the average low burning rate in Table II and obtaining the value 1.7. Calculating the corresponding ratio for average total particulate mass concentrations using the data in Fig. 3 also gives 1.7. The correspondence between the burning rate and particulate mass concentration implies a constant soot fraction for underventilated conditions.

A summary of the results for both fuels is given in Table II. These data are the result of burning many cups of fuel in each case, and thus the mass burning rates are average values. The HEPA filters tested with PS had protective metal face screens (1- by 1-cm mesh size) with the exception of filters number 6 and 7. The HEPA filters tested with PMMA all had the metal screens removed.

TABLE II

SUMMARY OF COMBUSTION PRODUCT PLUGGING OF HEPA FILTERS

Fuel	Test No.	Clean Static Pressure Drop (cm w.g.)	Apparent Mass Burning Rate (g/min)	Total Particulate Mass Collected at Plugging[a] (g)
PS	1	2.1	19.4 (high)	527
PS	2	2.1	21.3 (high)	432
PS	3	2.1	15.4 (low)	1256
PS	4	2.0	21.7 (high)	405
PS	5	2.1	17.5 (low)	1207
PS	6	2.1	22.9 (high)	432
PS	7	2.1	21.3 (high)	391
PMMA	8	2.2	11.6 (high)	233
PMMA	9	2.2	12.4 (low)	257
PMMA	10	2.2	15.6 (high)	186
PMMA	11	2.2	13.4 (low)	309

[a]The HEPA filter resistance ratio has a value of 12.0 for each filter.

The details of the plugging process for each filter are shown in Fig. 4. The actual resistance is normalized by the initial clean filter resistance (W_o = Initial R in Fig. 4). The data show the influence of the PS mass burning rate on the quantity of the particulate material collected that is necessary for plugging. For a given combustion condition (fuel type and mass burn rate), the following functional form is seen to correlate the plugging data

$$W/W_o = (1 + \alpha M_p + \beta M^2_p) \quad , \tag{14}$$

where W/W_o is the filter airflow resistance ratio, M_p is the accumulated particulate mass on the HEPA filter (grams), and the variables α and β are determined to give the best fit to the data. From Fig. 4, the importance of the protective screen on HEPA filter plugging can be seen to be negligible. Table III shows the values for α and β for the combustion conditions tested. The resistance ratio is observed to be a strong function of the linear term in M_p--the β values are relatively small. The filter plugging coefficients given in Table III can be used in the input data deck of the Los Alamos fire accident analysis computer code FIRAC.[15] This code is designed to model and predict fire-induced flows and thermal and material transport within complex nuclear fuel cycle facilities.

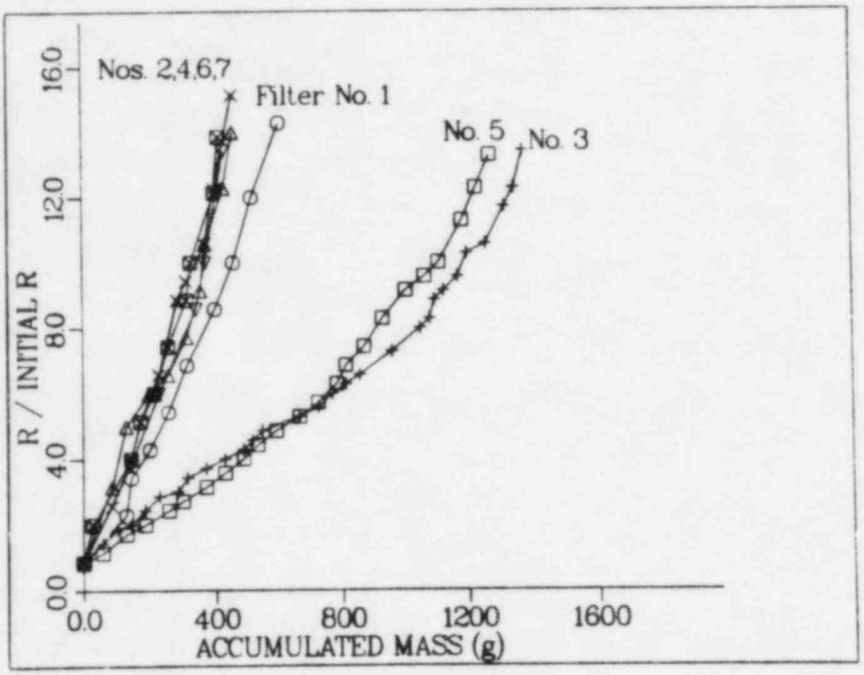

Fig. 4.
Variation of resistance ratio with accumulated mass for polystyrene combustion.

TABLE III

COMPILATION OF HEPA FILTER RESISTANCE RATIO FUNCTION[a] COEFFICIENTS

Fuel	Combustion Condition	α	β
PS	High O_2	0.022248	0.64249×10^{-6}
PS	Low O_2	0.0057105	0.17108×10^{-5}
PMMA	Underventilated	0.0476796	-0.30826×10^{-4}
PMMA	Overventilated	0.0641064	-0.57276×10^{-4}

[a]The HEPA filter resistance ratio has a value of 12.0 for each filter.

Particle size data can be used to explain the variation in PS combustion particulate mass necessary to plug the HEPA filters. From Table II, the mean total mass collected by the filters when nearly plugged (resistance ratio = 12) for the low and high burning rates are 1232 and 437 g, respectively. Table IV presents particle size data for both fuels. These data were obtained using the cascade impactors with sampling during the combustion of individual cups of fuel. The quantities in Table IV include the particulate mass concentration for particles larger than 2.0 μm ($\rho_{p\ell}$), the particulate mass concentration for particles smaller than 2.0 μm (ρ_{ps}), the total fuel mass burned (M_f), and the mass burning rate (m_f). Combining these into the ratio $\rho_{p\ell}M_f/m_f$ yields a parameter that modifies the concentration according to the combustion rate. The ratio of this parameter for those particles greater than 2.0 μm gives the value 2.7 when the average value of this parameter for high mass burning rate is divided by the low mass burning rate average value. When the corresponding ratio for accumulated particulate mass gains for the filter at the flow resistance ratio value of 12.0 is computed using the data of Table II, the number is 2.8. Numbers this close for these two ratios indicate that the particles greater than 2.0 μm in diameter dominate the plugging of the filter. Particles less than 2.0 μm apparently penetrate the filter medium, contributing to the mass of collected particulate material but contributing little to increase the static pressure drop

TABLE IV

COMBUSTION PARTICULATE MASS CHARACTERIZATION

Fuel	Combustion Condition	$\rho_{p\ell}$ (>2 μm) (g/m^3)	ρ_{ps} (<2 μm) (g/m^3)	M_f (g)	$\dot{m}_f$ (g/min)	$\rho_{p\ell}M_f/\dot{m}_f$	$\rho_{ps}M_f/\dot{m}_f$
PS	High O_2	0.051	0.074	186.6	20.1	0.47	0.69
PS	High O_2	0.059	0.050	223.8	22.2	0.59	0.50
PS	Low O_2	0.012	0.081	207.1	11.7	0.21	1.4
PS	Low O_2	0.0094	0.052	223.3	13.3	0.19	0.87
PMMA	Underventilated	0.0022	0.014	600.5	12.0	0.11	0.70
PMMA	Underventilated	0.0027	0.013	600.0	11.5	0.14	0.68
PMMA	Overventilated	0.0018	0.0031	1003.5	12.3	0.15	0.25
PMMA	Overventilated	0.0013	0.0035	1000.0	11.7	0.11	0.30

across the filter. Removal of the HEPA filters from the test apparatus supports this speculation because the upstream face had a thick "mat" of fragile particulate material that tended to fall away from the filter even when disturbed by the most careful handling.

B. PMMA Combustion and HEPA Filter Plugging

Figure 5 gives the particle aerodynamic diameter size distributions determined by cascade impactors directly upstream from the test HEPA filter. With the combustion of the PMMA fuel, the low burning rate particle size distributions are consistent, but the high burning rate distributions are apparently different. However, the burning rate does influence the particle size distribution.

Also indicated in Fig. 5 are the particulate mass concentrations associated with each condition. In contrast to the PS combustion characteristics, the average fuel mass burn rate (Table II) is not correlated with the airborne average particulate mass concentration. (See Fig. 5.) The mass burn rate ratio of the two conditions is only 0.9, and the mass concentration ratio is greater

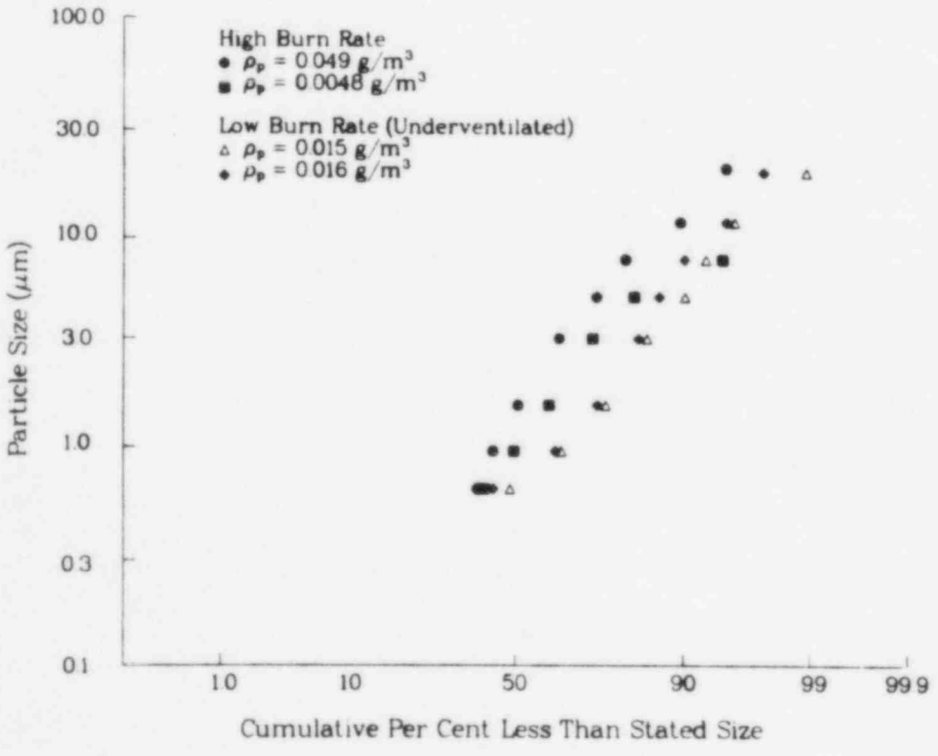

Fig. 5.
Polymethylethacrylate combustion particulate mass size distribution.

than 3. This is true because the low burn rate corresponds to underventilated combustion conditions and the high burn rate corresponds to overventilated conditions--the soot fractions are different.

Four HEPA filters were plugged with the PMMA combustion products; Tables II--IV and Fig. 6 show the results. All four of the HEPA filters had the protective metal screen removed, and the last filter (number 11) incorporated asbestos separators within the filtration media in place of the aluminum separators used in all the previous filters. Figure 6 shows that HEPA filter number 11 displays essentially normal behavior regarding plugging, indicating that the separator material does not discernibly influence the plugging characteristics for PMMA combustion products. Equation (14) again successfully correlates the filter resistance ratio in terms of M_p for the two PMMA combustion conditions.

Table IV suggests that the parameter $\rho_p \ell M_f/m_f$ (which was successful with the PS plugging data) is not successful for the PMMA tests. The corresponding parameter ($\rho_{ps} M_f/m_f$) ratio with the underventilated values divided by the overventilated values yields the number 2.5. The average accumulated masses on the filter causing plugging at a resistance ratio of 12 are 210 and 283 for the

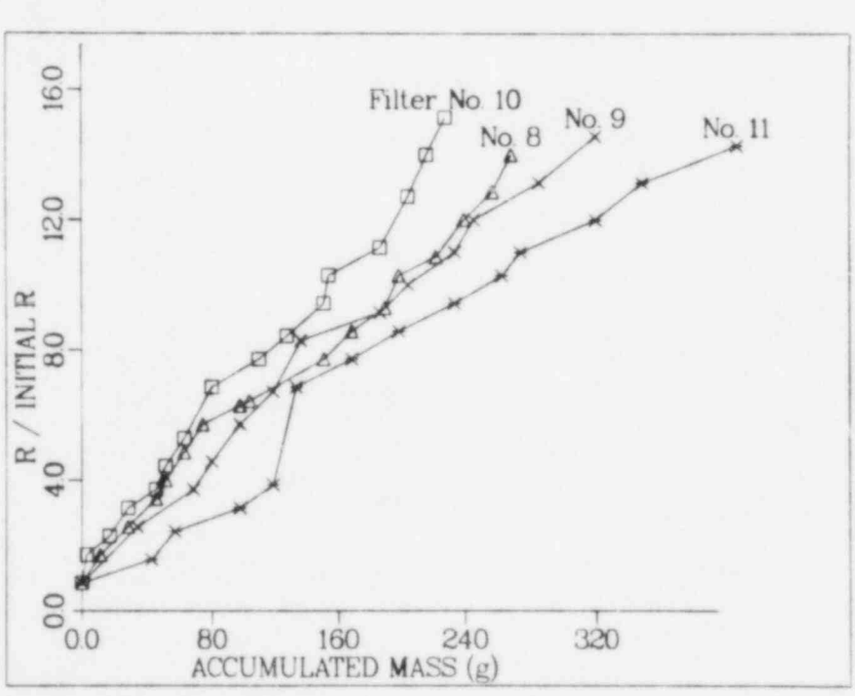

Fig. 6.
Variation of resistance ratio with accumulated mass polymethymethacrylate combustion.

overventilated to underventilated mass burning rates. The ratio of the overventilated to underventilated HEPA filter accumulated masses is 0.74. Consequently, this parameter is not appropriate for the PMMA tests. Rather, the corresponding particulate mass concentration for particles greater than 2.0 μm wnen divided yields a value of 1.04. This implies that again the larger particles are important for a HEPA filter's plugging characteristics. Additionally, going back to the PS data and using the same ratio of $\rho_{D\ell}$ gives a value 5.0, which is approximately double the HEPA filter mass gain ratio and thus is not appropriate.

IV. CONCLUSIONS

The test results quantitatively establish HEPA filter plugging characteristics for PS and PMMA combustion aerosols. These tests were performed to support development of the Los Alamos FIRAC fire accident analysis computer code. Tentative qualitative conclusions can be made regarding the plugging characteristics involving particulate mass concentration and accumulated particulate mass on the filter.

- Normalized HEPA filter flow resistance can be correlated with the accumulated mass gain on the filter for a given combustion aerosol (PS and PMMA). When the combustion conditions change (fuel and/or oxygen availability), the HEPA filter plugging characteristics change and are explained with the particulate mass concentration for particles greater than 2.0 μm.
- The lower the fuel soot fraction, the smaller the accumulated mass gain on the HEPA filter required for plugging. This results from the physical characteristics of the particulate material--mass concentration and particle size.

REFERENCES

1. P. A. F. White and S. E. Smith, High Efficiency Air Filtration (Butterworths, London, 1964).
2. M. K. W. Chan, "Testing and Calibration Results of the Filex Smoke Generators," Pacific Northwest Laboratory draft report (March 30, 1982).

3. A. Tewarson, "Physico-Chemical and Combustion/Pyrolysis Properties of Polymeric Materials," Factory Mutual Research Corporation (Norwood, Massachusetts) technical report RC80-T-79 (1980)

4. W. Strauss, Industrial Gas Cleaning (Pergamon Press, Ltd., Oxford, 1966), pp. 214-243.

5. M. W. Thring and W. Strauss, "The Effects of High Temperature on Particle Collection Mechanisms," Trans. Inst. of Chemical Engineers 41, 248 (1963).

6. C. N. Davies, Air Filtration (Academic Press, London, 1973).

7. C. N. Davies, Ed., Aerosol Science (Academic Press, London, 1966).

8. C. A. Snyder and R. T. Pring, "Design Consideration in Filtration of Hot Gases," Ind. Eng. Chem. 47, 960 (1955).

9. C. Tien, C. Wang, and D. T. Barot, "Chainlike Formation of Particle Deposits in Fluid Particle Separation," Science 196, 983-986 (1966).

10. W. Bergman, A. H. Bierman, H. Hebard, B. Lum, and W. D. Kuhl, "Electrostatic Filters Generated by Electric Fields," Lawrence Livermore National Laboratory preprint UCRL-84878 (January 1981).

11. J. J. Dallman, "An Investigation of the Simulated Combustion Aerosol Loading of HEPA Filters," Masters Thesis, New Mexico State University (1982).

12. D. L. Fenton, J. J. Dallman, P. R. Smith, R. A. Martin, and W. S. Gregory, "The Los Alamos National Laboratory/New Mexico State University Filter Plugging Test Facility--Description and Preliminary Results," Los Alamos National Laboratory report in preparation.

13. C. A. Burchsted, A. B. Fuller, and J. G. Kahn, "Nuclear Air Cleaning Handbook," Energy Research and Development Administration Handbook ERDA-76-21 (1976).

14. R. A. Martin and D. L. Fenton, "Full-Scale Measurements of Smoke Transport and Deposition in Ventilation System Ductwork," Los Alamos National Laboratory report in preparation.

15. R. W. Andrae, J. W. Bolstad, R. D. Foster, W. S. Gregory, F. R. Krause, R. A. Martin, and P. K. Tang, "FIRAC User's Manual," Los Alamos National Laboratory report in preparation.

DISTRIBUTION

	Copies
Nuclear Regulatory Commission, RI, Bethesda, Maryland	173
Technical Information Center, Oak Ridge, Tennessee	2
Los Alamos National Laboratory, Los Alamos, New Mexico	50
Total:	225

NRC FORM 335 (6-83) U.S. NUCLEAR REGULATORY COMMISSION

BIBLIOGRAPHIC DATA SHEET

1 REPORT NUMBER (Assigned by TIDC and Vol. No. if any)
NUREG/CR-4264
LA-10436-MS

2 Leave blank

3 TITLE AND SUBTITLE
Investigation of High-Efficiency Particulate Air Filter Plugging by Combustion Aerosols

4 RECIPIENT'S ACCESSION NUMBER

5 DATE REPORT COMPLETED
MONTH: April YEAR: 1985

6 AUTHOR(S)
D.L. Fenton*, M.V. Gunaji*, W.S. Gregory, and R.A. Martin
* Mechanical Engineering Department, New Mexico State University, Las Cruces, NM 88003

7 DATE REPORT ISSUED
MONTH: May YEAR: 1985

8 PERFORMING ORGANIZATION NAME AND MAILING ADDRESS (Include Zip Code)
Los Alamos National Laboratory
Los Alamos, NM 87545

9 PROJECT/TASK/WORK UNIT NUMBER

10 FIN NUMBER
A7029

11 SPONSORING ORGANIZATION NAME AND MAILING ADDRESS (Include Zip Code)
Division of Risk Analysis
Office of Nuclear Regulatory Research
U.S. Nuclear Regulatory Commission
Washington, DC 20555

12a TYPE OF REPORT
Informal Report

12b PERIOD COVERED (Inclusive dates)

13 SUPPLEMENTARY NOTES

14 ABSTRACT (200 words or less)

Experiments were conducted to investigate high-efficiency particulate air (HEPA) filter plugging by combustion aerosols. These tests were done to obtain empirical data to improve our modeling of filter plugging phenomena using the Los Alamos National Laboratory fire accident analysis code FIRAC. Commercially available 0.61-m by 0.61-m square filters were tested in a specially designed facility to determine how airflow resistance varies with increased filter loading by combustion aerosols. Two organic fuels normally found in nuclear fuel cycle facilities, polystyrene (PS) and polymethylmethacrylate (PMMA), were burned under varied conditions to generate combustion aerosols. The test facility included a combustor, a 23-m-long duct, and a specially designed gravimetric balance for determining the aerosol mass gain of the filters.

Test results include correlations of HEPA filter resistance ratios (actual resistance/initial resistance) with aerosol mass gain. The mass gain of plugged HEPA filters was found to correlate with the airborne mass concentration of material in the size range greater that approximately 2.0 μm. Also, the fuel with a smaller soot fraction, PMMA, produced filter plugging at lower accumulated aerosol mass deposits on or within the filter.

15a KEY WORDS AND DOCUMENT ANALYSIS

15b DESCRIPTORS

16 AVAILABILITY STATEMENT
Unlimited

17 SECURITY CLASSIFICATION (This report)
Unclassified

18 NUMBER OF PAGES

19 SECURITY CLASSIFICATION (This page)
Unclassified

20 PRICE
$

Available from

Superintendent of Documents
U.S. Government Printing Office
Post Office Box 37082
Washington, D. C. 20013-7982

and

National Technical Information Service
Springfield, VA 22161

Los Alamos